CRYSTAL GROWTH & DESIGN

THE UNIVERSITY OF MEMPHIS
University Libraries

Subscriber access provided by University Libraries, University of Memphis

Article

Understanding the role of water in different solid forms of Avibactam sodium and its affecting mechanism

Zhiyong Ding, Wei Su, Xin Huang, Beiqian Tian, Xiaowei
Cheng, Yafei Mao, Guiping Li, Han Liu, and Hongxun Hao

Cryst. Growth Des., **Just Accepted Manuscript** • DOI: 10.1021/acs.cgd.9b01459 • Publication Date (Web): 10 Jan 2020

Downloaded from pubs.acs.org on January 15, 2020

Just Accepted

"Just Accepted" manuscripts have been peer-reviewed and accepted for publication. They are posted online prior to technical editing, formatting for publication and author proofing. The American Chemical Society provides "Just Accepted" as a service to the research community to expedite the dissemination of scientific material as soon as possible after acceptance. "Just Accepted" manuscripts appear in full in PDF format accompanied by an HTML abstract. "Just Accepted" manuscripts have been fully peer reviewed, but should not be considered the official version of record. They are citable by the Digital Object Identifier (DOI®). "Just Accepted" is an optional service offered to authors. Therefore, the "Just Accepted" Web site may not include all articles that will be published in the journal. After a manuscript is technically edited and formatted, it will be removed from the "Just Accepted" Web site and published as an ASAP article. Note that technical editing may introduce minor changes to the manuscript text and/or graphics which could affect content, and all legal disclaimers and ethical guidelines that apply to the journal pertain. ACS cannot be held responsible for errors or consequences arising from the use of information contained in these "Just Accepted" manuscripts.

is published by the American Chemical Society. 1155 Sixteenth Street N.W.,
Washington, DC 20036

Published by American Chemical Society. Copyright © American Chemical Society.
However, no copyright claim is made to original U.S. Government works, or works
produced by employees of any Commonwealth realm Crown government in the course
of their duties.

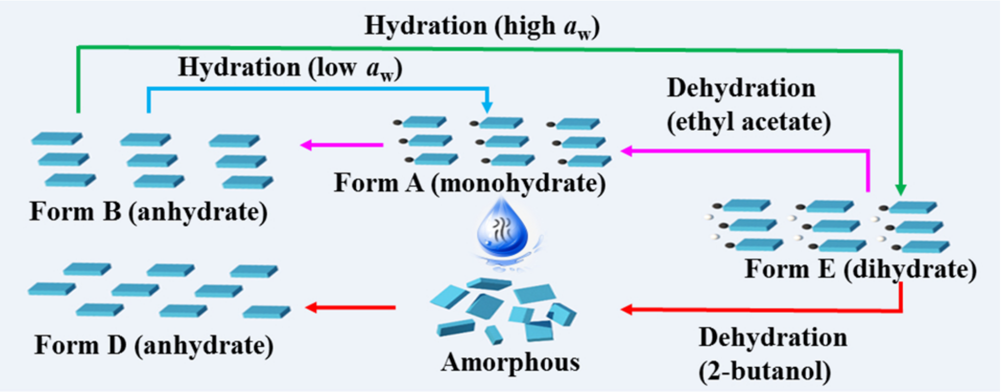

In this study, to reveal the role of water in the formation and dehydration of hydrates, the effect of water activity on the formation of hydrates as well as the mechanism of disintegration of water molecules from crystal lattice was investigated by using Avibactam sodium as model compound.

88x34mm (300 x 300 DPI)

Understanding the role of water in different solid forms of Avibactam sodium and its affecting mechanism

Zhiyong Ding,[†] Wei Su,[†, ‡] Xin huang,[†, ‡] Beiqian Tian,[†] Xiaowei Cheng,[†] Yafei Mao,[†] Guiping Li,[†] Han Liu,[†] and Hongxun Hao[*, †,‡]

[†] School of Chemical Engineering and Technology, Tianjin University, Tianjin 300072, China

[‡] Collaborative Innovation Center of Chemical Science and Engineering (Tianjin), Tianjin 300072, China

ABSTRACT

Hydrates are common in pharmaceutical development and the formation of hydrates will affect the performance of the final product. However, the role of water playing in crystal packing remains unclear. In this study, Avibactam sodium, which has one dihydrate (Form E), one monohydrate (Form A) and two anhydrous forms (Form B and D), was chosen as the model compound to understand this subject. Single crystal structures of four solid forms were obtained and characterized by single X-ray diffraction. The Dynamic Vapor Sorption experiments revealed the moisture-dependent stability increased in the order: Form B < Form D < Form A < Form E. It can be envisaged that the integration of water molecules could noticeably compensate the potential intermolecular interactions, thereby significantly improving the crystal stabilities of hydrates. Furthermore, the hydration of Form B was investigated to understand the integration of water molecules by measuring the critical hydration water activities (a_w). The results indicated that both water activities and temperature are vital factors to determine the amount of water molecules existing in crystal lattice. Moreover, to probe the disintegration of water molecules, the dehydration of dihydrate was investigated in detail by solid-state transformation and solvent-mediated transformation experiments. Finally, “Two-step Dehydration” and “One-step Dehydration + Recrystallization” mechanisms of these different pathways were proposed by analyzing the transformation experiments results and the crystal structure of various solid forms.

KEYWORDS: Avibactam sodium, polymorph, hydrate, hydration, water activity, crystal structure, dehydration, mechanism

INTRODUCTION

Polymorphs, solvates as well as hydrates are highly prevalent occurrence and are of great importance in pharmaceutical industry.[1, 2] Generally, different solid forms of the same compound exhibit different physicochemical properties, such as dissolution rate, stability, flowability and solubility, which could affect the final quality of medical products directly.[3-5] In recent years, hydrates have drawn more and more attentions of a significant number of crystal engineers.[6] Statistical investigations have manifested that more than one-third of compounds could exist in the form of hydrates.[7] The different physicochemical properties of hydrate can be used to change the drug release rate or stabilize the formulation with the extra advantage of nontoxic compared with other solvates.[8] It can be readily envisaged that the compensation to potential intermolecular interactions, the decreasing of void space and the increasing of packing efficient in crystal could promote the formation of hydrates.[9-11] Besides, water molecules possess excellent hydrogen bonds donors and acceptors, which leads to the formation of multiple interactions with API molecules. Hence, the ubiquitous water provides probability to the presence of numerous hydrates.

Hydration or dehydration processes may occur unexpectedly during drug development, manufacturing, storage and pharmaceutical preparation and could affect the qualities of the final products.[12, 13] Hence, it is of great significance to investigate the relative stabilities of the hydrates and figure out the phase transformation processes between hydrates and corresponding neat forms.[14-19] Previous studies have indicated that the stability of hydrates is closely related to the humidity, water activity in solvent circumstance and temperature.[20, 21] Liu et al.[22] investigated the transformation water activity and concluded that the transformation water activity ratio of different crystal forms of theophylline was inversely proportional to the solubility ratio at certain temperature. Ito et al.[8] found that the anhydrate of antibiotic clarithromycin reversibly transformed to dihydrate when RH increased to 60%, and then transited to trihydrate at 95% RH. Zhang et al.[23] reported that two new polymorphs of Huperzine A were acquired by slurring and heating dehydration from the same hydrate, respectively. Terada et al.[24] demonstrated that the order of dehydration is determined by the hydrogen bonds circumstance in two independent water channels in the dihydrate of lisinopril. Although these works have discussed the form transformation processes of hydrates, the mechanism of integration and disintegration of water molecules from crystal lattice is not well understood so far.

In this study, to reveal the role of water in the formation and dehydration of hydrates, the effect of water activity on the formation of hydrates as well as the mechanism of disintegration of water molecules from crystal lattice was investigated by using Avibactam sodium as model compound. Avibactam sodium is a novel β-lactamase inhibitor. [25] Its chemical structure is presented in Figure 1. In the structure of Avibactam sodium, Na^+ could form coordination bonds with water molecules easily. Besides, there are several O atoms serving as hydrogen bonds acceptors and $-NH_2$ acting as hydrogen bond donor. For these reasons, Avibactam sodium is prone to crystallize into hydrous forms and the abundant intermolecular interactions make it an ideal model compound for investigating the role of water molecules in crystal packing. To achieve that goal, single crystals of four Avibactam sodium solid forms were disclosed, including one monohydrate (Form A), and two anhydrous forms (Form B and D), and one dihydrate (Form E). Hirshfeld surface analysis was performed to further compare the molecular interaction of various solid forms. Then, the moisture-dependent stability and thermal-dependent stability of different solid forms and the preferential solid form were evaluated using dynamic vapor sorption (DVS), differential scanning calorimetry (DSC) and thermogravimetric analysis (TGA). Furthermore, the critical water activity at a series of temperatures was determined to understand the influence of the water activity and temperature on the hydration process. Finally, two different dehydration processes by solution-mediated phase transformation (SMPT) in ethyl acetate and 2-butanol were investigated in detail, respectively.

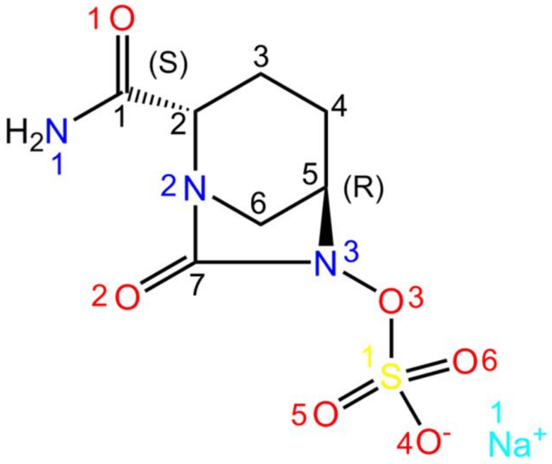

Figure 1. Molecular structure of Avibactam sodium.

EXPERIMENTAL SECTION

Materials. Avibactam sodium with purity higher than 99% used in the present work was supplied by Qilu Tianhe Pharmaceutical Co. Ltd. (Jinan, China). All analytical grade solvents, including ethyl acetate, 1-propanol, ethanol, acetone, 2-butanol were purchased from Kemiou Chemical Reagent Co., Ltd.

Preparation of different crystal forms. The polymorph screening trials include evaporation,[26] cooling crystallization,[27] slurry crystallization,[28] antisolvent precipitation,[28] liquid-assisted grinding experiments[29] and crystallization with additives.[30, 31] Finally, four crystal forms were obtained, including one monohydrate (Form A), one dihydrate (Form E) and two kinds of neat-forms (Form B and Form D).

Powder X-ray Diffraction Analysis. Powder X-ray Diffraction (PXRD) was used to identify samples on Rigaku D/max-2500 (Rigaku) using Cu Kα radiation (0.15405 nm) in 2θ range of 2-35° and scanning speed rate of 8°/min.

Single crystal X-ray diffraction (SCXRD). The single crystals of Avibactam sodium were all obtained by using the solvent evaporation method (detailed procedures in supporting information). Single crystal X-ray diffraction (SCXRD) measurements were conducted on Rigaku Saturn 70 CCD diffractometer using

Mo-Kα radiation (λ = 0.71073 Å) with graphite monochromator. Integration and scaling of intensity data were accomplished using the SAINT program. The structures were solved using the SHELXS-2014 suite of programs, and refinement was conducted using SHELXL-2018. Anisotropic displacement parameters were refined for all non-hydrogen atoms. All hydrogen atoms were located by Fourier-difference synthesis and fixed geometrically according to the environment with pre-defined isotropic thermal factors. Data were corrected considering the effects of absorption using SADABS. [32]

Thermal Analysis. Differential Scanning Calorimetry measurements were conducted in DSC 1/500 (Mettler Toledo., Switzerland) with a dry nitrogen purge flow of 100 mL·min^{-1}. About 5-10 mg crystalline powder samples were placed into aluminum pans and analyzed with a temperature range from 300 to 540 K. TGA was performed in TGA/DSC STAR^{ev} System (Mettler Toledo., Switzerland) with a nitrogen purge flow of 20 mL·min^{-1}. The measurement temperature range was from 300 to 540 K. The heating rate was both set as 10 K·min^{-1} for TGA and DSC.

Dynamic Vapor Sorption (DVS). The water sorption/desorption experiments of four crystal forms of Avibactam sodium were performed on a dynamic vapor sorption analyzer (VTI-SA, VTI Corporation, USA). The experiments were implemented over a relative humidity (RH) range of 5 to 95% by the step of 10%. The RH was maintained until the weight change is less than 0.01 wt.% per minute or the maximum step length is 60 minutes. The temperature was set at 298.15 K and solid forms were analyzed by PXRD after experiments.

Determination of critical water activity. The critical water activity (a_w) needed by the hydration of Form B was ascertained by slurring the solid of Form B in the mixture of water and 1-propanol with various water activities. A series of mixed solvents with different water mole fractions (x_w = 0.03, 0.05, 0.07, 0.1, 0.15, 0.2, 0.3, …, 0,9) were prepared. Excess of Form B solid was added into ≥ 5 ml mixed solvents and stirred for 12 h to reach equilibrium. Then, the wet cakes were withdrawn and analyzed using PXRD. The experiments were performed at varying temperature (288.15, 293.15, 298.15, 303.15, 308.15 ±0.1 K). The a_w was calculated according to the Wilson Equation as implemented in the ASPEN Properties program.[33]

Solid-state dehydration of monohydrate and dihydrate. The solid-state dehydration behaviors of Form A and Form E were observed under hot-stage microscope (HSM, Olympus UMAD3). The sample was heated from 293.15 to 393.15 K with a heating rate of 5 $K\cdot min^{-1}$. Photos were recorded at certain time intervals using polarized light microscope.

Solvent mediated dehydration of dihydrate. The presaturated solution concerning Form B (or Form D) was prepared at 293.15 K. About 0.5 g solid of Form B (or Form D) was added into 40 ml ethyl acetate (or 2-butanol) and stirred with magnetic stirrer for 24 h. Then, the suspension was allowed to standing for 6 h and then supernatant was filtered with 0.22 μm filter. 1 g solid of dihydrate was added into crystallizers with 20 mL presaturated solution at 293.15 K. Samples of crystals were immediately filtered every 15 minutes and dried under vacuum. The dried solids were characterized by PXRD and SEM.

RESULTS AND DISCUSSION

Identification and characterization of different crystal forms. One monohydrate form, one dihydrate form, and two anhydrate form of Avibactam sodium were obtained. Polarizing microscopy images show that various forms exhibit different crystal habits (Figure 2). Form A is block-like crystal while Form B and Form D both have rectangular plate shape and Form E shows short rod shape. The PXRD patterns of four solid forms of Avibactam sodium are presented in Figure 3. The diffraction peak positions of these four crystal forms are consistent with the reported forms in the patents.[34, 35]

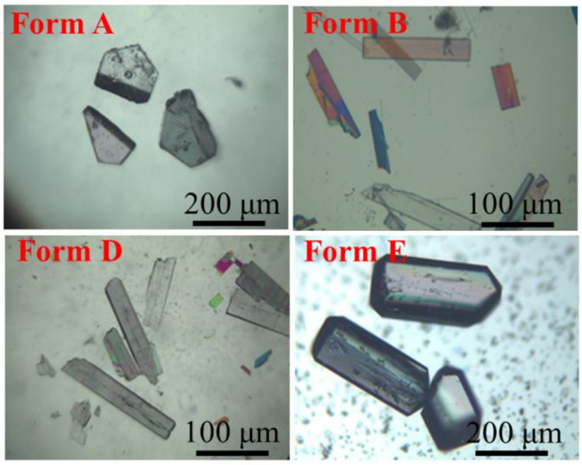

Figure 2. Polarizing microscopy images of the single crystals of Form A, Form B, Form D and Form E.

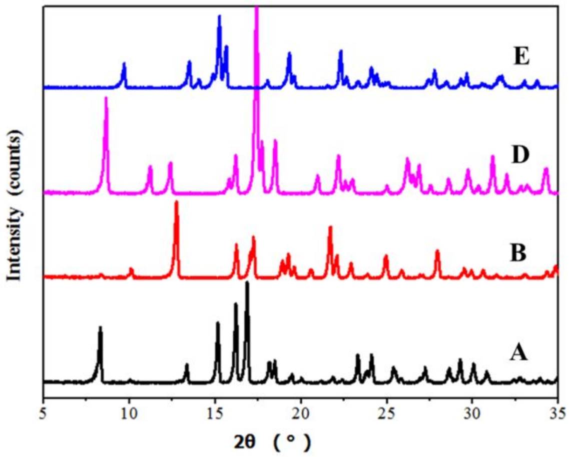

Figure 3. PXRD patterns of four crystal forms of Avibactam sodium.

Crystal Structure Analysis. The crystal structures of different Avibactam sodium forms including monohydrate (Form A), anhydrous phases (Form B and D) and dihydrate (Form E), were successfully determined to understand the changes of molecular interactions caused by the integration of water molecules. The crystallographic data are summarized in Table 1. The asymmetric units of the four solid forms are shown in Figure S1 and the intermolecular H-bonding parameters are presented in Table S1. All the peaks displayed in the measured patterns of the bulk powder closely matched those in the simulated patterns generated from the single crystal diffraction data (Figure S2, Supporting Information), confirming the formation of highly pure phases.

Table 1. Crystallographic Data Of Avibactam Sodium

Name	**Form A**	**Form B**	**Form D**	**Form E**
Formula	$C_7H_{10}N_3NaO_6S{\cdot}H_2O$	$C_7H_{10}N_3NaO_6S$	$C_7H_{10}N_3NaO_6S$	$C_7H_{10}N_3NaO_6S{\cdot}2H_2O$
Molecular Weight	305.25	287.23	287.23	323.26
Temperature/K	296.15	113.15	113.15	113.15
Crystal System	monoclinic	monoclinic	monoclinic	orthorhombic
Space Group	$P2_1$	$P2_1$	$P2_1$	$P2_1\,2_1\,2_1$
a (Å)	8.6213(17)	8.5289(17)	8.0823(16)	7.7815(16)
b (Å)	6.9281(14)	6.2868(13)	6.4168(13)	12.374(3)
c (Å)	10.391 (2)	10.219(2)	10.434(3)	12.931(3)
α (deg)	90	90	90	90
β (deg)	91.82 (3)	93.77(3)	104.13(3)	90
γ (deg)	90	90	90	90
Cell volume (Å^3)	620.30 (2)	546.75(19)	524.76(19)	1245.1(4)
Z	2	2	2	4
ρ_{clac} (g cm^{-3})	1.634	1.745	1.818	1.724
R_{int}	0.0296	0.0589	0.0309	0.0349
Final R indexes [$I \geq 2\sigma(I)$]	0.0260	0.0331	0.0246	0.0248
wR_2	0.0674	0.0633	0.0639	0.0605
GOF (S)	1.052	0.9090	1.044	1.019
CCDC	1962393	1962394	1962395	1962396

The crystal system of Form A is monoclinic with the space group of $P2_1$. There are one molecule of Avibactam sodium and one molecule of water in the asymmetric unit (Figure S1), making it monohydrate. The arrangement of water molecules is shown in Figure 4. As we can see from Figure 4a, two Avibactam sodium molecules and two water molecules are linked together to construct a ring by forming coordinate bonds with Na^+ ions. These rings are further connected via coordinate bonds one by one, and then extend along *a*-axis to form an infinite chain (Figure 4b). In addition, one Na^+ ion form coordinate bonds with six oxygen atoms (two O1 of amide groups from two adjacent Avibactam sodium molecules, O4 and O5 of sulfate groups, two Ow atoms from two water molecules) and one nitrogen atom (N2 from heterocyclic ring). These chains are allowed to expand along *ab* plane and form 2D layers through these coordinate bonds. In addition,, there are plenty of H-bonds formed by water and Avibactam sodium molecules (including N1-H···O6 (N···O, 2.98 Å), Ow-H···O2 (O···O, 2.83 Å), Ow-H···O5 (O···O, 2.78 Å)), making the 2D layers more stable. Finally, these 2D layers are stacked along the *c*-axis (Figure 4c) by the connection of hydrogen bonds (N1-H···O6, 3.01 Å) between amino group and sulfate group from upper and lower layers. The final packing pattern of Form A is shown in Figure 4d.

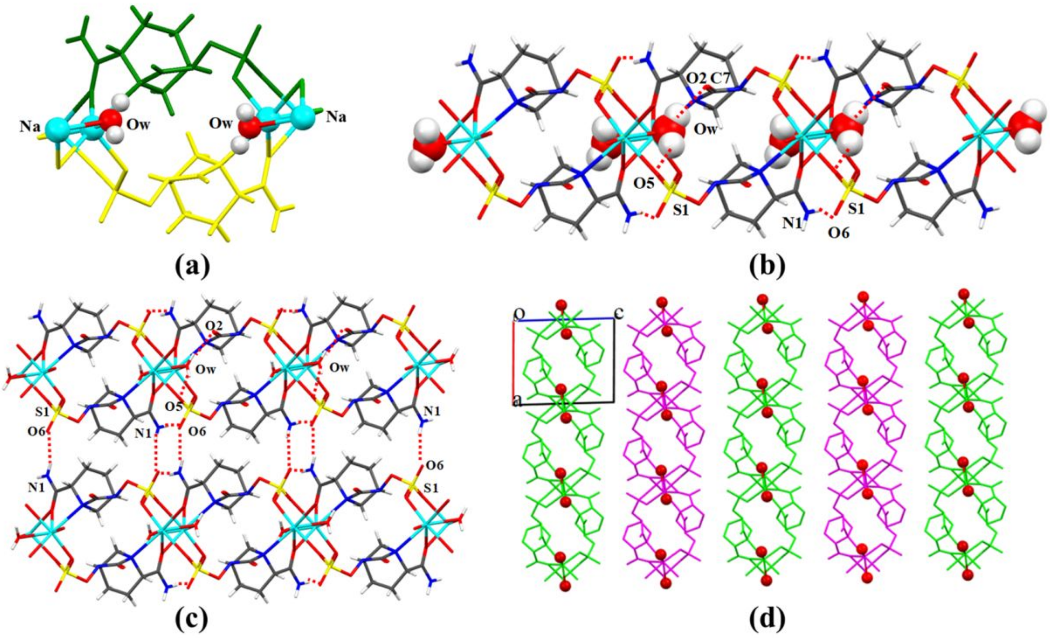

Figure 4. (a) The structure of the ring in Form A. (b) The arrangement of H_2O. (c) The hydrogen bonds network between two layers, viewed along the *b*-axis. (d) 3D packing patterns of Form A (different colors represent different 2D layers and bright red ball represents the O atoms of water molecule), the H atoms are omitted for clear view.

Form B belongs to $P2_1$ space group with one molecule in the asymmetric unit. Interestingly, the crystal packing of Form B is very similar to the monohydrate phase (Form A). As shown in Figure 5a, the basic building block of Form B is a ring consisting of two Avibactam sodium molecules. The ring is connected by coordinate bonds between O atoms (O1 of amide group, O2 of carbonyl group, O3, O4, O5 and O6 of sulfate groups) and Na^+ ions. It is obvious that the rings of Form B lack water molecules when compared to the rings of Form A. Moreover, these rings also expand and form 2D layer along *ab* plane. These layers are further stacked via H-bonds along *c*-axis [(N1-H···O4, 3.16 Å), (N1-H···O5, 3.19 Å), (N1-H···O2, 3.35 Å)], as shown in Figure 5b. The crystal structure of Form B viewed along *b*-axis is shown in Figure 5c.

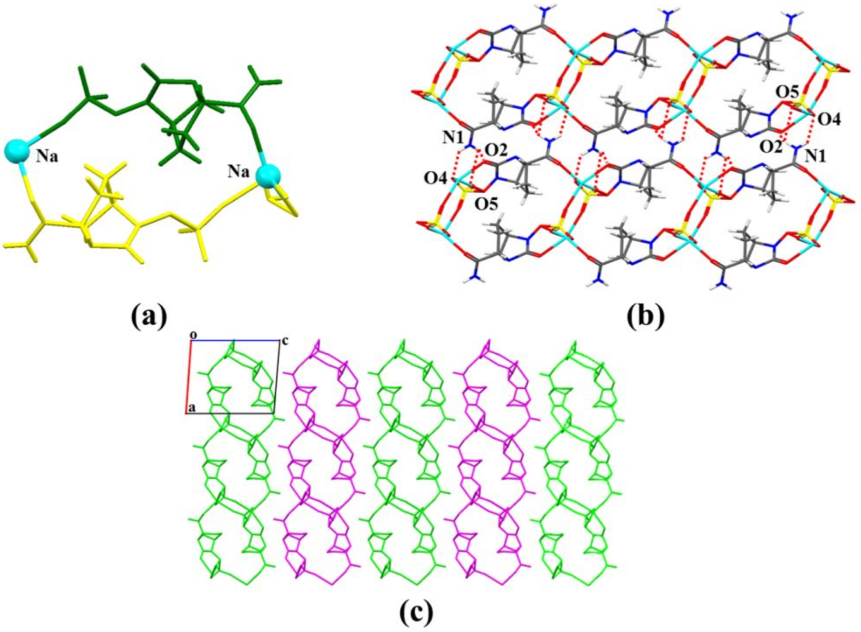

Figure 5. (a) The structure of the ring in Form B. (b) The hydrogen bonds between two layers in Form B, viewed along the *b*-axis. (c) 3D packing patterns of Form B (different colors represent different 2D layers). The H atoms are omitted for clear view.

Similar with Form A and B, the crystal system of Form D is also monoclinic with space group $P2_1$, and there is only one Avibactam sodium molecule in the asymmetric unit. However, “sandwich-shaped” sheets are formed in which Na$^+$ ions combine two slices of Avibactam sodium molecules via coordinate bonds, as shown in Figure 6a. Besides the coordinate bonds with Na$^+$ ions in the sheets, the amino groups and sulfate groups of adjacent Avibactam sodium also participate in the formation of H-bonds [(N1-H···O3, 3.27 Å), (N1-H···O6, 2.99 Å)] to stabilize the sheets structure (Figure 6b). Therefore, these sheets are allowed to further expand via H-bonds (N1-H···O5, 3.08 Å) between amino groups and sulfate groups from two sheets, as shown in Figure 6c. Finally, the 3D packing structures of Form D are constructed and the corresponding patterns are shown in Figure 6d.

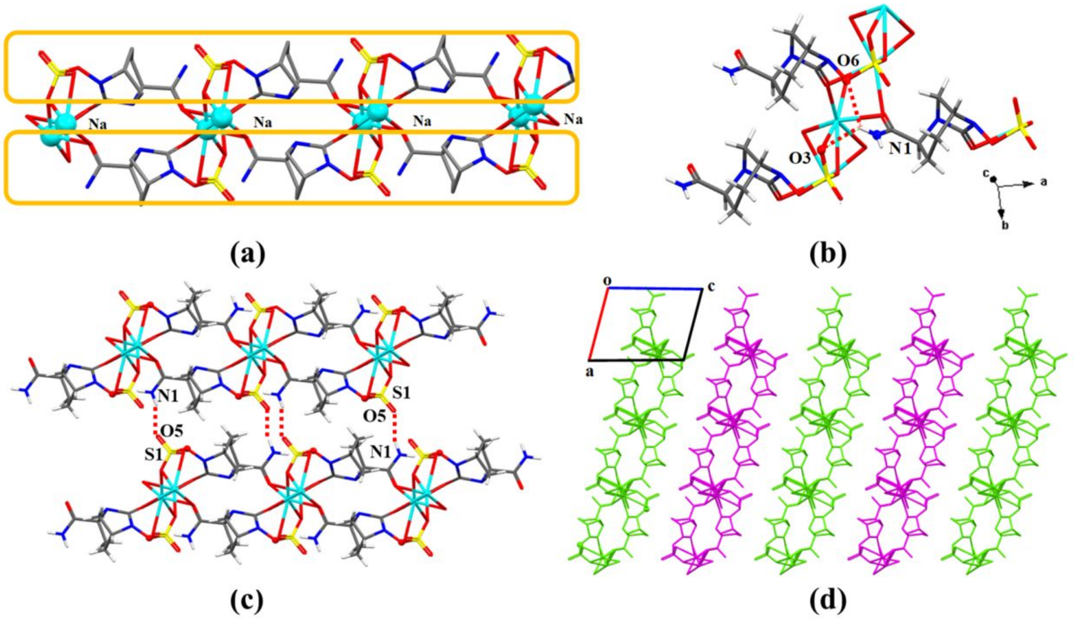

(a) (b)

(c) (d)

Figure 6. (a) “Sandwich” structure of sheets in Form D. (b) The hydrogen bonds in the sheets. (c) The hydrogen bonds network between two sheets in Form D, viewed along the *b*-axis. (d) 3D packing patterns of Form D (different colors represent different 2D sheets), the H atoms are omitted for clear view.

Form E belongs to orthorhombic system with space group of $P2_12_12_1$, and include two water molecules and one Avibactam sodium molecule in asymmetric unit. It can be seen that two kinds of water molecules are combined into the crystal lattice by different ways: H_2O (1) is connected with three different hydrogen bonds [N1-H···Ow1 (N···O, 2.82 Å), Ow1-H···O4 (O···O, 2.78 Å), and Ow1-H···Ow2 (O···O, 2.86 Å) (red dashed lines in Figure 7a)]. However, H_2O (2) is linked to Na^+ ion by strong coordinate bonds and it also forms three H-bonds with the O atoms of Avibactam sodium and H_2O (1) [Ow2-H···O6 (O···O, 2.86 Å), Ow2-H···O5 (O···O, 2.84 Å), and Ow1-H···Ow2 (O···O, 2.86 Å) (red dashed lines in Figure 7b)]. Moreover, NH_2– which is an excellent H-bonding donor also forms three H-bonds with oxygen atoms [N1-H···Ow1 (N···O, 2.82 Å), N1-H···O4 (N···O, 3.08 Å), and N1-H···O6 (N···O, 3.40 Å) (red dashed lines in Figure 7c)]. Besides that, every Na^+ ion forms coordinate bonds with five oxygen atoms (two O1 of amide group from two adjacent Avibactam molecules, O2 from carbonyl group, O4 from sulfate group, Ow2 from H_2O (2)) and one nitrogen atom (N2 from heterocyclic ring). As we can see in Figure S3, plenty of channels along *c*-axis are also formed. The molecules of H_2O (1) are arranged neatly in channels along the *c*-axis by H-bonds in order to occupy these channels and reduce the voids in crystal structure. It’s worth noting that the sophisticated hydrogen bonds networks have a significant influence on stabilizing the crystal structure of Form E. Finally, the hydrogen bonding network and the stable crystal structure of Form E is shown in Figure 7d.

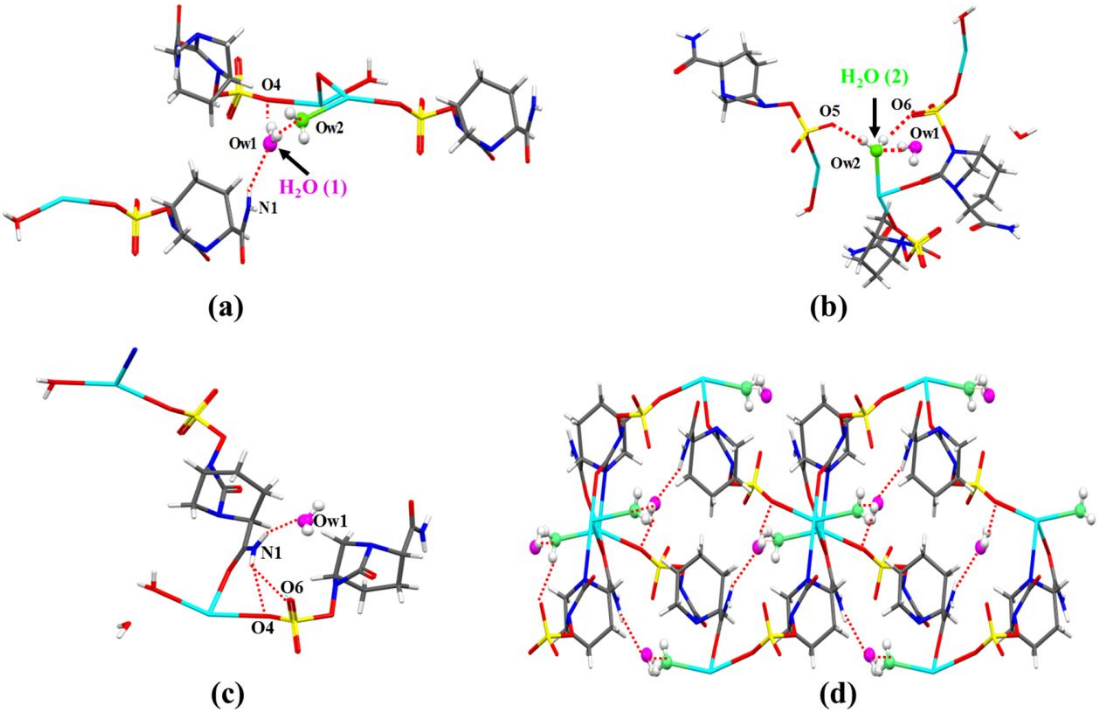

Figure 7. Hydrogen bonding patterns in Form E. (a) The hydrogen bonds of H_2O (1). (b) The hydrogen bonds of H_2O (2). (c) The N–H···O interactions between two neighbor Avibactam sodium molecules as well as Avibactam sodium and H_2O (1). (d) Hydrogen bonding network of Form E. For clear view, the O atoms of H_2O (1) and H_2O (2) are shown as ball-stick style with highlighting in magenta and light green, respectively.

Hirshfeld surface analysis. The Hirshfeld surface analysis is a useful tool for encoding information about dominant intermolecular interactions in crystal.[36, 37] The subtle packing differences among different solid forms can be interpreted in Hirshfeld surface plot (Figure S4) and 2D fingerprint plots (Figure 8a). As illustrated in Figure 8a, the strikes of Form A which represent hydrogen bonds extend down to (di, de) = (0.8, 1.2) (corresponding to the H-bond distance of 2.0 Å). The length of H-bonds in Form B and D are significantly longer than Form A with minimum (di, de) = (1.0, 1.4) and (di, de) = (0.9, 1.2), respectively. However, the strikes of Form E extend down to (di, de) = (0.7, 1.1) (corresponding to the H-bond distance of 1.8 Å), which means that the introduce of water molecules in crystal lattice lead to stronger hydrogen bonds and more stable structure. The relative contributions of each interaction to the

Hirshfeld surface are depicted in Figure 8b. It is obvious that the two hydrates Form A and Form E are mainly stabilized by H···O/O···H-N, O···H-O/O-H···O hydrogen bonds, Na-O as well as Na-N coordinate bonds and H-H contacts. In contrast, Na-N coordinate bonds and O-H···O hydrogen bonds are absent in the two anhydrates Form B and Form D.

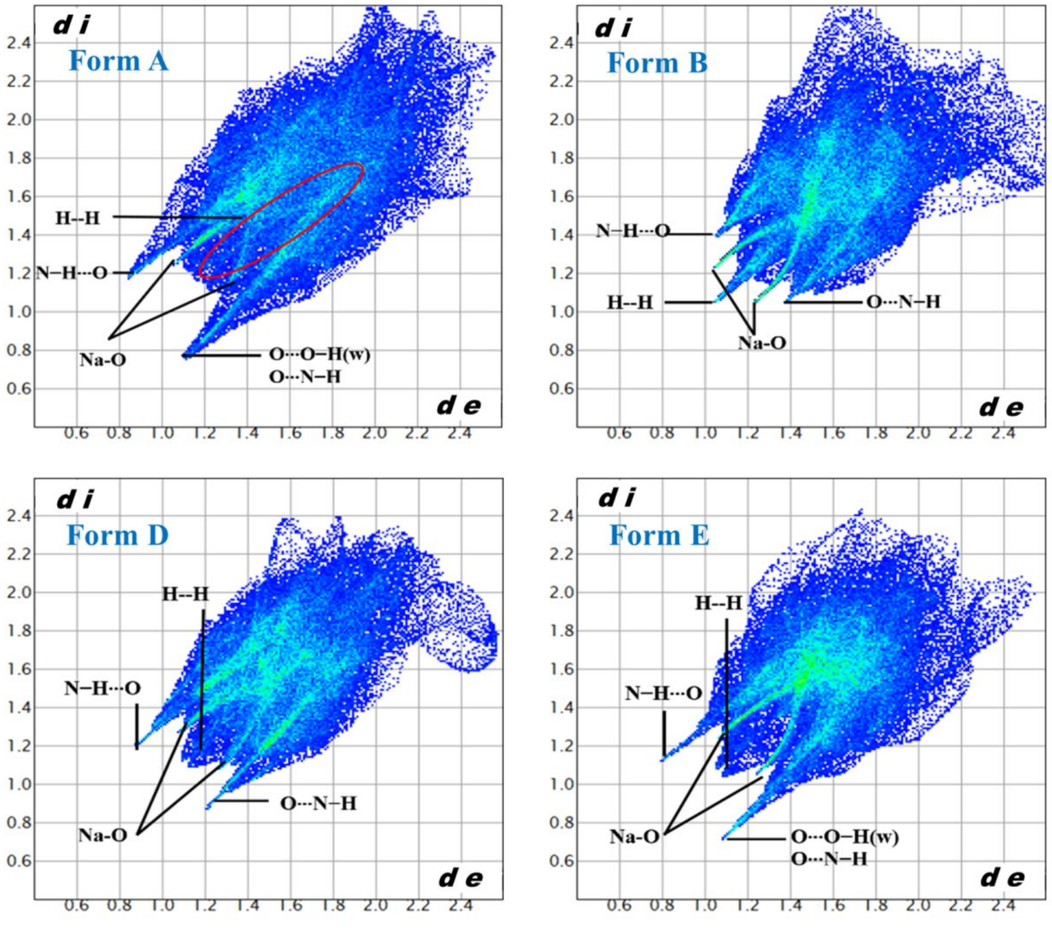

(a)

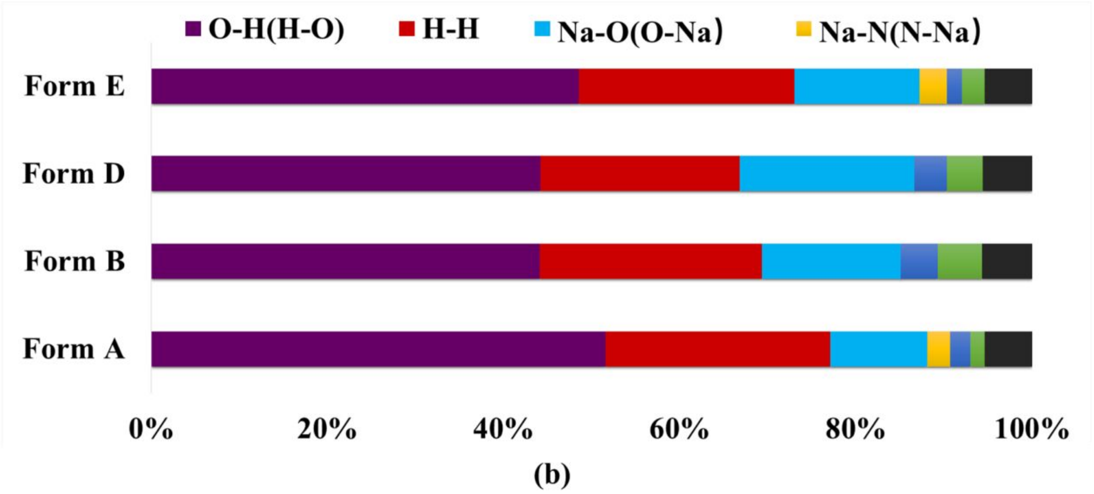

Figure 8. (a) 2D fingerprint plots of Form A, Form B, Form D and E. (b) The relative contribution of different interactions to the Hirshfeld surface.

Stability analysis. To further explore the effect of the introduction of water molecules on crystal stabilities, a thorough evaluation of the stability of various solid forms is extremely important in the drug development process. Among all the factors that could affect stability, temperature is a crucial one, especially for hydrates. In this part, DSC and TGA were performed to study thermal-dependent stability of four crystal forms of Avibactam sodium, the results are shown in Figure 9. It can be seen that Form A showed a mass loss of 5.76% with an endothermic peak at 378 - 389 K, which confirmed Form A is monohydrate (calculated value: 5.90%). Subsequently, decomposition of Form A was observed at 510 K with the weight loss of 36% , corresponding a big exothermic peak in DSC. As seen from TGA thermograms, there was no weight loss for Form B and Form D below 500 K. DSC data of both forms exhibit negligible exothermal or endothermal peak in this temperature range, which means that these two polymorphs are anhydrous forms. As temperatures rise, Form B and Form D showed mass loss of 33.65% and 35.42% with two sharp exothermic peaks at 510 K and 502 K resectively, which are confirmed to be the decomposition of two solid forms. It can be preliminarily considered that Form B is more thermodynamically stable than Form D. As for Form E, the weight loss of TGA is 11.20%, which is consistent with the calculated value (11.11%) for the dehydration of two water molecules from this dihydrate. Morever, Form E shows similar decomposition temperature with Form A and Form B at about 509 K. Correspondingly, Form E shows two endothermal peaks at 359 - 372 K and 375 - 391 K in DSC data respectively, indicating the dehydration process was two steps rather than one-step. The first peak corresponds to the escape of the water molecules ($H_2O(1)$) connected only by hydrogen bonds. The second peak represents the detachment of water molecules ($H_2O(2)$) which form coordinate bonds with Na^+ ions. This conclusion can also be verified by PXRD analysis after heating the crystal of Form E to 372 K (and 398 K), respectively (Figure S5).

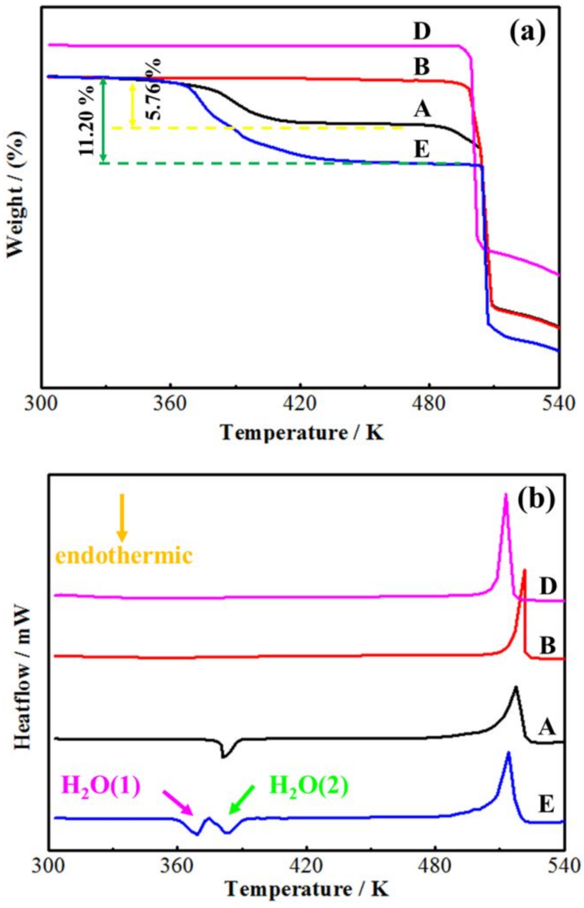

Figure 9. Comparison of thermal analysis figures of Forms A, Form B, Form D and Form E of Avibactam sodium. (a) TGA analysis (10 K·min^{-1}). (b) DSC analysis (10 K·min^{-1}).

Apart from temperature, moisture is another important factor affecting the stability of drug solid forms, especially for hydrates. In this part, the moisture sorption/desorption experiments were conducted by determining both the weight change (using DVS) and the phase composition (using PXRD) of the samples to investigate the moisture-dependent stability of four crystal forms of Avibactam sodium.

The DVS diagrams results of the four solid forms are shown in Figure 10. It can be seen from Figure 10a that Form A exhibited excellent moisture-dependent stability as the weight kept constant in the 0 – 85% RH range. When the RH reached 95%, Form A adsorbed water and showed a slight weight increase of about 6%. Then, dihydrate was obtained with the RH decreasing to 85%, which was confirmed from the PXRD patterns after the DVS experiment (Figure S6a). However, the moisture sorption/desorption isotherms of Forms B showed a two-step stoichiometric hydration. As shown in Figure 10b, the first hydration process of Form B occurred at 70 - 85% RH with a weight gain of 6.2%. This is consistent with the formation of monohydrate Form A, which was also confirmed by PXRD (Figure S6b). It indicates the first hydration of Form B has a low energy barrier, proving that crystal structures of these two forms are likely to be similar. Then, the mass change of solid kept rising to 21.2% with RH reaching to 95%. When RH was decreased to 80%, the mass increase reduced to 12.1%, which is consistent with the formation of dihydrate Form E. Unlike Form B, anhydrate Form D converted to dihydrate directly. As shown in Figure 10c, Form D was stable in the RH range of 0 – 80%. Form D began to adsorb water and showed a pronounced weight increase of about 15% when the RH reached 95%. Then, the mass increase reduced to 12.4% as RH was decreased to 80% again. Finally, PXRD results showed that the resulting phase after the DVS experiment remained was dihydrate Form E, as shown in Figure S6c. The great difference of crystal structures makes Form D cannot transform to Form A by increasing the relative humidity. It is interesting that the weight of Form E only increased by 4% when RH increased to 95%, as shown in Figure 10d. The high moisture-dependent stability of Form E may be due to the strong coordinate bonds as well as abundant H-bonds between the water molecules and the API molecules. It is obvious that the moisture-dependent stability increased in the order: Form B < Form D < Form A < Form E. It can be concluded that the integration of water molecules leads to strong coordinate bonds as well as abundant H-bonds between the water and the API molecules. These H-bonds could compensate to potential intermolecular interactions of anhydrates, thereby significantly improving the crystal stability of hydrates.

However, it is insufficient to confirm the relative stabilities of Form B and Form D only by thermal analysis and moisture sorption/ desorption experiments. To further compare the relative stability of these two anhydrates, mixed suspension phase transformation method was employed. 1: 1 (wt.%) mixture of two anhydrates crystal was stirred in four kinds of pure solvents (1-propanol, ethanol, acetone, 2-butanol) at 283.15 K, 303.15 K, 323.15 K and 343.15 K for about 1 week. The results of slurry experiments are given in Table S2. The results showed that the mixture of Form B and Form D transformed into Form B in all solvents. According to Ostwald rules, if the metastable polymorph continues to interact with a bulk solution for a period of time, the metastable polymorph would dissolve and a more stable polymorph would nucleate and grow. Therefore, it can be concluded affirmatively that Form B is more thermodynamically stable than Form D.

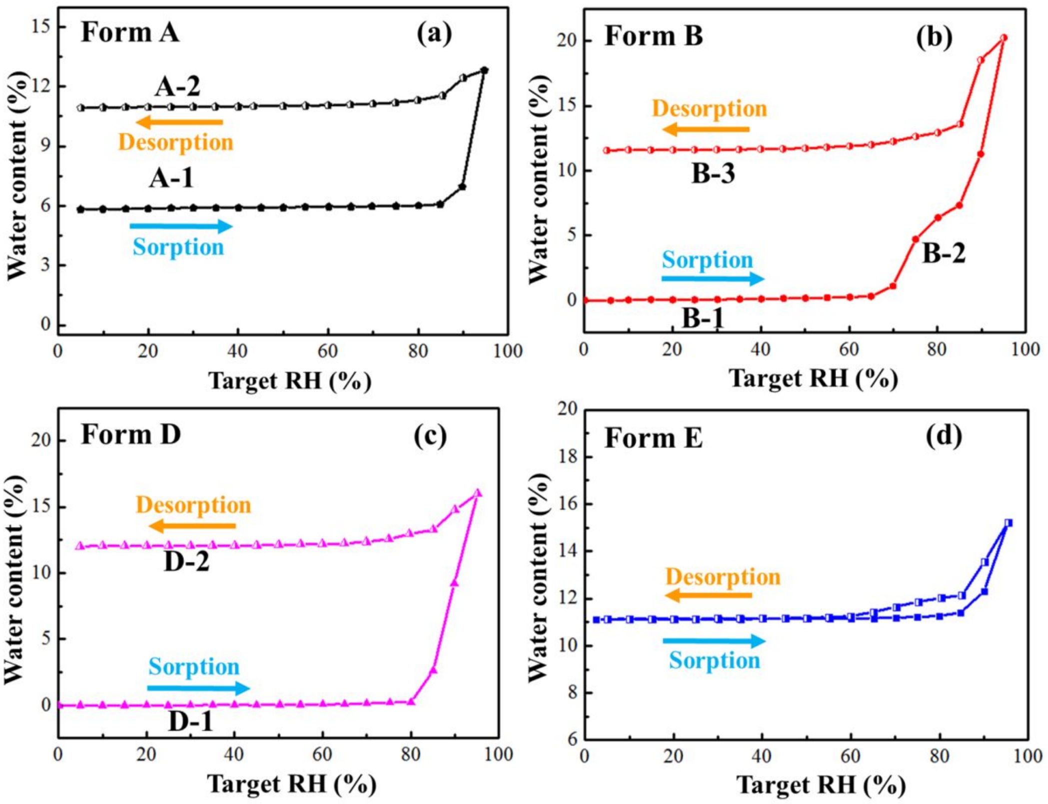

Figure 10. DVS diagrams of four solid forms of Avibactam sodium: (a) Form A (b) Form B (c) Form D (d) Form E. A-1, B-1 and D-1 are the materials of Form A, Form B and Form D, respectively. B-2 is the Form B samples collected at RH = 85%. A-2, B-3 and D-2 are the samples collected respectively when the DVS experiments were finished.

Mechanism of the hydration. As discussed above, both moisture and temperature are critical factors which could affect the presence of hydrates. However, DVS experiments can only show the solid-solid transformation between hydrates and anhydrous forms. To further figure out the influence of moisture and temperature on the integration of water molecules into crystal lattice of hydrates, the solution-mediated hydration experiments were conducted in water and 1-propanol mixtures with different water activities. Because of the two-step hydration and better thermodynamic stability than Form D, Form B was chosen for the object of this study. The critical hydration water activity (a_w) of Form B was given in Table S3, and $a_{\mathrm{w(B\text{-}A)}}$ and $a_{\mathrm{w(B\text{-}E)}}$ represent the critical water activity required for the transformation from

Form B to Form A and Form E, respectively. It can be seen that a_w increased gradually with the rising of temperature which indicated the increasing difficulty of the hydration of Form B. Besides, the thermodynamic stability ranges were also visualized in Figure 11. Taking the 288.15 K for instance, when water activity (a_w) $\leq$ 0.1374, Form B (anhydrate) is the most stable form and is the only phase at equilibrium. With the increase of water activity, Form A (monohydrate) appears. When water activity (a_w) values lie between 0.1374 and 0.2374, Form A becomes the only phase at equilibrium. However, Form E (dihydrate) is the most stable form when $a_w \geq 0.2374$. Thus, 0.1374 and 0.2374 are the critical hydration water activities of Form A and Form E respectively.

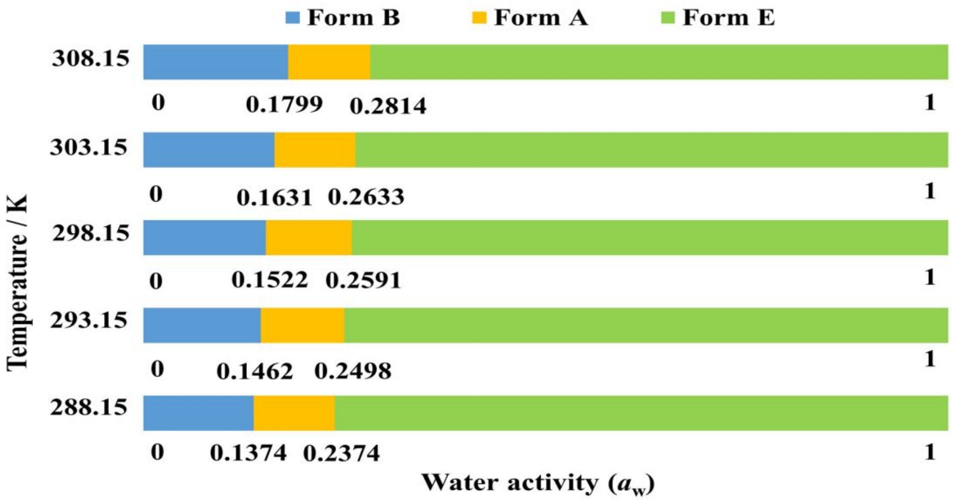

Figure 11. The thermodynamic stability ranges of Form B, Form A and Form E.

Thus, it is obvious that the critical water activity has a strong dependence on temperature and it could be correlated with the mechanism of the hydration. During the solution mediated hydration, the formation of hydrate from anhydrous crystal include two steps: the dissolution of anhydrate and the nucleation and growth of hydrate. This process could be expressed in the following equilibrium:

$$X(solid)+mH_2O \overset{K_1}{\rightleftharpoons} [X]+mH_2O \overset{K_2}{\rightleftharpoons} X\cdot mH_2O(solid) \qquad (1)$$

Based on the law of chemical equilibrium, K_1 and K_2 can be expressed as Eq. 2.

$$K_1 = \frac{a[X]}{a[X(solid)]} \tag{2}$$

$$K_2 = \frac{a[X \cdot mH_2O(solid)]}{a[X]a[H_2O]^m} \tag{3}$$

where *m* is the numbers of H_2O in crystal lattice; *X* (solid) and $X{\cdot}mH_2O$ (solid) represent the anhydrate crystal (Form B: m=0) and corresponding hydrates (Form A: m=1 and Form E: m=2), respectively. $a[H_2O]$ represents critical hydration water activity. If the standard states of unit activity of X(solid) and $X{\cdot}mH_2O$(solid) are represented by their pure solid phases, the a[X(solid)] and $a[X{\cdot}mH_2O(solid)]$ are all equal to 1.

$$K_h = K_1K_2 = \frac{a[X \cdot mH_2O(solid)]}{a[X(solid)]a[H_2O]^m} = a[H_2O]^{-m} \tag{4}$$

where K_h represents the equilibrium constant of hydration equation.

According to Van't Hoff equation:

$$\ln K_h = -m \ln a_w = -\frac{\Delta H^\theta}{RT} + \frac{\Delta S^\theta}{R} \tag{5}$$

Then divide both side by -m,

$$\ln a_w = \frac{\Delta H^\theta}{mRT} - \frac{\Delta S^\theta}{mR} \tag{6}$$

where R is gas constant (R=8.314).

The relationship of the critical hydration water activity and temperature was calculated. What's more, ΔH^Θ and ΔS^Θ were estimated using experimental data which represent the hydration enthalpy and entropy respectively. The obtained parameters of Van't Hoff equations are given in Table 3 and the following equations could be obtained.

$$\ln a_{w(B-A)} = -\frac{9546.13}{RT} + \frac{16.54}{R} \tag{7}$$

$$\ln a_{w(B-E)} = -\frac{11588.7}{2RT} + \frac{16.35}{2R} \tag{8}$$

The results shows that $\Delta H^\Theta_{(B\text{-}A)}$= -9546.13 J·mol^{-1} and $\Delta S^\Theta_{(B\text{-}A)}$= -16.54 J·(mol·K)$^{-1}$, whereas $\Delta H^\Theta_{(B\text{-}E)}$= -11588.7 J·mol^{-1} and $\Delta S^\Theta_{(B\text{-}E)}$= -16.35 J·(mol·K)$^{-1}$. The linear fitting curves of the relationship between $1/T$ and the ln a_w are shown in Figure 12, which demonstrated good fitting result. In addition, crystal morphology also changed considerably at various water activity (Figure S7). It indicates that regulation of water activity is an ideal tool to manipulate the result of crystallization and improve the properties of crystal.

Table 3. The thermal data of the hydration of Avibactam sodium Form B.

	ΔH^{Θ} / J·mol^{-1}	**ΔS^{Θ} / J· (mol·K)$^{-1}$**
Form B → Form A	-9546.13	-16.54
Form B → Form E	-11588.7	-16.35

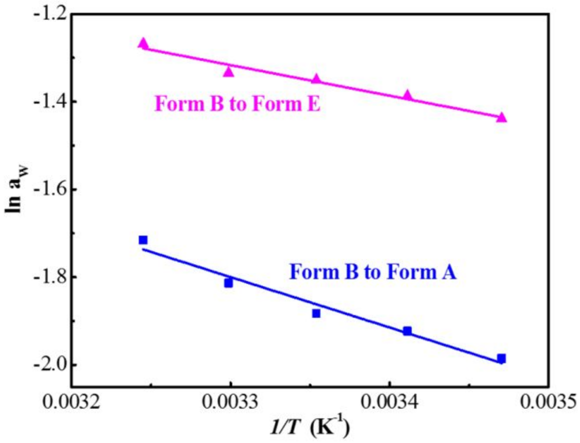

Figure 12. The critical water activity and its temperature dependence of Avibactam sodium anhydrates and hydrates in the equilibrium state of the 1-propanol/ water system.

Dehydration of hydrates and its mechanism. To have a better understanding of how the water molecules escape from the crystal lattice, hot-stage microscopy was used to observe the change of single crystals of two hydrates during solid state dehydration process. The results are shown in Figure 13a. For monohydrate Form A, the formation of boundary was initiated at the defects of crystal and then extended towards both sides of crystal surface when temperature reached to 378.45 K, which means the escape of water molecules (Figure 13a). In other words, the dehydration began and the anhydrate started to nucleate and grow. The optical properties also changed during this dehydration process and the appearance of water drops indicated the accomplishment of the dehydration process. For Form E, as shown in Figure 13b, a clear boundary on the surface of the crystal was initially observed and then propagated through the whole crystal when Form E was heated to 369.35 K. It indicates that the first category of water molecules combined only by H-bonds began to escape from the crystal lattice and Form E converted to Form A (Figure S5). Then, little drops of water on the edge of crystal appeared when the temperature reached 385.45 K, which implied the start of the escape of the second type of water molecules connected by coordinate bonds as well as H-bonds from crystal lattice. At the same time, the crystal was completely blackened and the crystal lattice of Form A was collapsed.

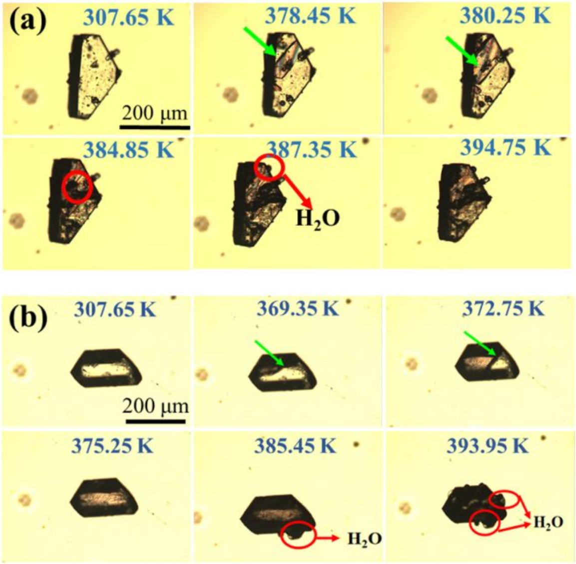

Figure 13. Hot stage microscopy images of the solid-state dehydration of Form A (a) and Form E (b) during the heating process.

Apart from solid-state dehydration, solution-mediated dehydration by slurring the hydrate in solvents was also investigated in detail. The PXRD patterns as well as the SEM images during the dehydration process of Form E are shown in Figure 14 and 15. The detailed transformation process in ethyl acetate can be illustrated as follows: firstly, the rod-shaped Form E crystals started to break and the brick crystal continued to nucleate and growth after putting the dihydrate crystals (Form E) into ethyl acetate for 4 hours (Figure 15a). At the same time, the characteristic peaks of Form E at 2θ of 9.7° and 22.2° began to decrease and peaks at 2θ of 8.3°and 16.7° started to emerge and increase, which was confirmed to be the appearance of Form A. Then, the characteristic peaks of monohydrate disappeared gradually and anhydrate Form B started to appear after about 10 hours 25 minutes, as shown in Figure 14a. The whole process was very slow and it would take 12 hours for dihydrate to lose two water molecules one by one.

However, the dehydration process in 2-butanol was significantly different from the pathway in ethyl acetate. As shown in Figure 14b and Figure 15b, the solid of dihydrate began to break and aggregate after adding the dihydrate crystals (Form E) in to 2-butanol for 2 hours 40 minutes. Correspondingly, the characteristic peaks of Form E broadened and the peak intensities decreased gradually. The crystal structure was totally destroyed and transformed to amorphous solid after 5 hours and the surface of Avibactam sodium became very rough and irregular. About 7 hours later, the amorphous solid would further recrystallize and the characteristic peaks of Form D would appear and become stronger. At the same time, the irregular appearance of the solid tended to become into plated-shaped.

Based on the crystal structures of various solid forms and dehydration processes, two different dehydration mechanisms of form E were proposed, as shown in Figure 16. The first mechanism is “Two-step Dehydration”, which was suitable for the dehydration process in ethyl acetate. During the first step of this transformation process, the intermolecular hydrogen bonds would be destroyed and the first type of water molecules which were connected only by H-bonds would escape from the crystal lattice. The molecular interactions, including H-bonds and coordinate bonds, would be further reorganized and monohydrate Form A will be formed. Then, the second category water molecules which formed coordination bonds and hydrogen bonds with Avibactam sodium molecules also began to run out of crystal. Finally, the second step transformation was completed and the anhydrous Form B was obtained.

On the contrary, the dehydration process of Form E in 2-butanol could be summarized to be "One-step Dehydration + Recrystallization" mechanism. Two types of water molecules would detach from the crystal lattice at a very short interval of time in this situation, which will lead to the collapse of crystal structure and the formation of amorphous solids. However, since the amorphous solid is not stable in solvent environment, the molecules of API would be rearranged to crystal with the continuous interaction with solvent. Therefore, Form D will be eventually obtained.

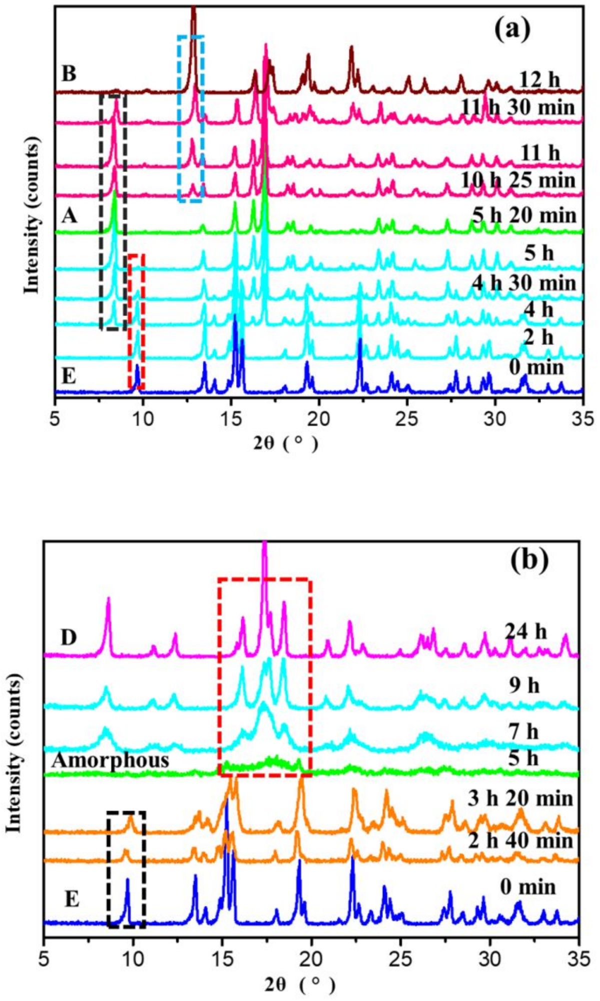

Figure 14. PXRD patterns during the dehydration process of Avibactam sodium Form E in two different solvents at 293.15 K. (a) In ethyl acetate. (b) In 2-butanol.

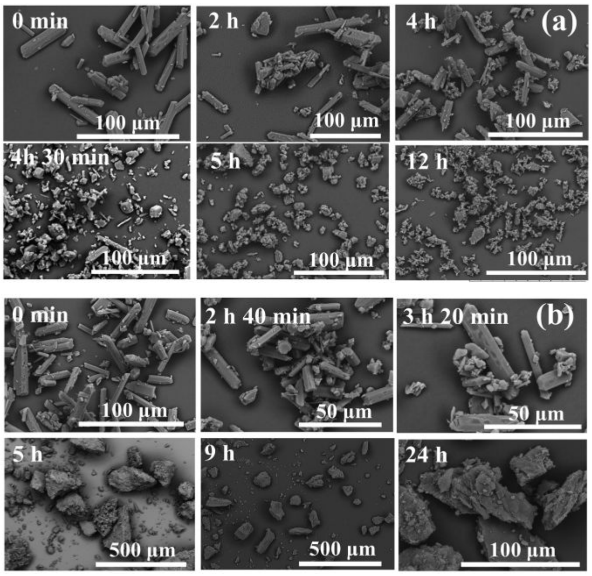

Figure 15. SEM pictures of crystals during the dehydration process of Avibactam sodium Form E at 293.15 K. (a) In ethyl acetate. (b) In 2-butanol.

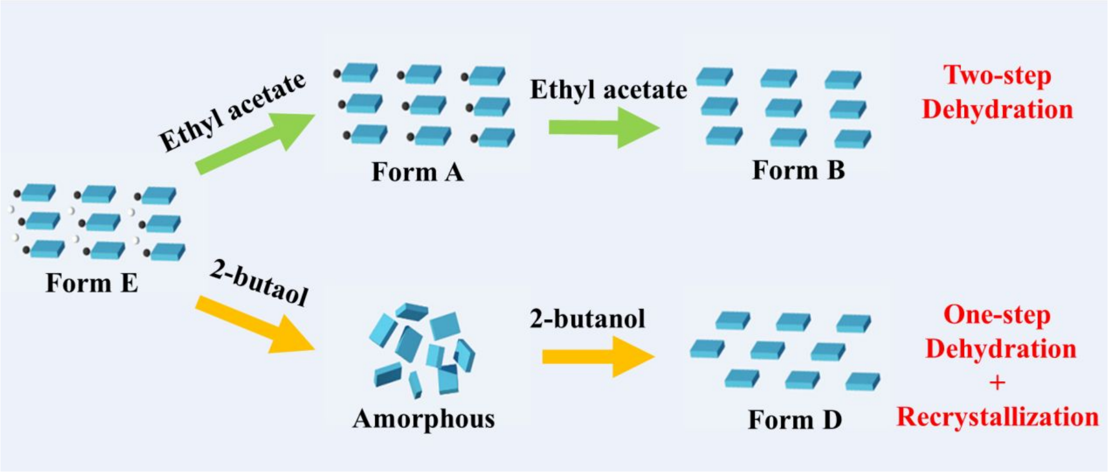

Figure 16. Proposed mechanism of for two different dehydration processes of Form E.

CONCLUSIONS

In this work, to reveal the role of water in the formation and dehydration of hydrates, the effect of water activity on the formation of hydrates as well as the mechanism of disintegration of water molecules from crystal lattice was investigated by using Avibactam sodium as model compound. Crystal structures of four different solid forms (including one monohydrate form (Form A), two anhydrous forms (Form B and D) and one dihydrate form (Form E)) of Avibactam sodium were successfully solved and analyzed. It is noticeable that Form A adopts an analogous assembly mode to Form B, whereas the former integrates one water molecule into asymmetric unit by coordinate bonds and hydrogen bonds. Form E combines another category water molecule with crystal lattice by hydrogen bonds based on the building block of Form A. However, the structure of Form D showed a wide difference with the other solid forms. The Dynamic Vapor Sorption experiments revealed the moisture-dependent stability increased in the order: Form B < Form D < Form A < Form E. It can be concluded that the integration of water molecules could stabilize the crystal structure of hydrates. The hydration of Form B in mixed solvents with various water activities was investigated to understand the integration of water molecules. The results indicate that the presence of hydrous state depends on water activity and temperature, and the integration of water molecules into crystal lattice will become more difficult as temperature increases. Moreover, the dehydration process of dihydrate was studied by solid-state dehydration using hot-stage microscopy and solution-mediated dehydration in two kinds of solvents. Interestingly, Form E first transformed to Form A and then transformed to Form B in ethyl acetate, which were consistent with the process of solid-state dehydration. However, the crystals of Form E slurring in 2-butonal underwent an amorphous state and then turned into Form D ultimately. Finally, "Two-step Dehydration" and "One-step Dehydration + Recrystallization" mechanisms of these different pathways were proposed by considering both the experimental results and the crystal structure of various solid forms.

ASSOCIATED CONTENT

Supporting Information

The Supporting Information is available free of charge on the ACS Publications website at:

- The preparation of single crystals; Asymmetric units of four solid forms; The simulated and experimented PXRD; Table of hydrogen bond data; Crystal packing in Form E; Hirshfeld surface; PXRD patterns of Form E at 303 K, 372 K and 398 K; RXPD patterns of Avibactam sodium solid forms before and after DVS experiment; The comparison results of relative stability between Form B and Form D; The Critical Hydration Water Activity of Form B; . Photos of crystals after the hydration of Form B. (PDF)

Accession Codes:

CCDC: 1962393	corresponding Form A in article
CCDC: 1962394	corresponding Form B in article
CCDC: 1962395	corresponding Form D in article
CCDC: 1962396	corresponding Form E in article

These four accession codes contain the supplementary crystallographic data for this paper. These data can be obtained free of charge via www.ccdc.cam.ac.uk/data_request/cif, or by emailing data_request@ccdc.cam.ac.uk, or by contacting The Cambridge Crystallographic Data Centre, 12 Union Road, Cambridge CB2 1EZ, UK; fax: +44 1223 336033.

AUTHOR INFORMATION

Corresponding Author

*Tel.: 86-22-27405754. Fax: +86-22-27374971.

E-mail: hongxunhao@tju.edu.cn

ORCID

Hongxun Hao: 0000-0001-6445-7737

Notes

The authors declare no competing financial interest.

ACKNOWLEDGMENTS

This research is financially supported by National Natural Science Foundation of China (No. 21978201 and No. 21908159).

REFERENCES

(1) Ayala, A. P.; Siesler, H. W.; Cuffini, S. L. Polymorphism incidence in commercial tablets of mebendazole: a vibrational spectroscopy investigation. *J. Raman Spectrosc.* **2008,** *39*, 1150-1157.

(2) Zhu, B.; Wang, J. R.; Ren, G. B.; Mei, X. F. Polymorphs and Hydrates of Apatinib Mesylate: Insight into the Crystal Structures, Properties, and Phase Transformations. *Cryst. Growth Des.* **2016,** *16*, 6537-6546.

(3) Albesa-Jove, D.; Pan, Z.; Harris, K. D. M.; Uekusa, H. A solid-state dehydration process associated with a significant change in the topology of dihydrogen phosphate chains, established from powder X-ray diffraction. *Cryst. Growth Des.* **2008,** *8*, 3641-3645.

(4) Braun, D. E.; McMahon, J. A.; Bhardwaj, R. M.; Nyman, J.; Neumann, M. A.; van de Streek, J.; Reutzel-Edens, S. M. Inconvenient Truths about Solid Form Landscapes Revealed in the Polymorphs and Hydrates of Gandotinib. *Cryst. Growth Des.* **2019,** *19*, 2947-2962.

(5) Cruz-Cabeza, A. J.; Davey, R. J.; Oswald, I. D. H.; Ward, M. R.; Sugden, I. J. Polymorphism in p-aminobenzoic acid. *CrystEngComm* **2019,** *21*, 2034-2042.

(6) Hao, H. X.; Yin, Q. X.; Zhong, J.; Wang, X. C. Crystallization for Pharmaceutical and Food Science. *Curr. Pharm. Des.* **2018,** *24*, 2327-2328.

(7) Aaltonen, J.; Strachan, C. J.; Pollanen, K.; Yliruusi, J.; Rantanen, J. Hyphenated spectroscopy as a polymorph screening tool. *J. Pharm. Biomed. Anal.* **2007,** *44*, 477-483.

(8) Ito, M.; Shiba, R.; Watanabe, M.; Iwao, Y.; Itai, S.; Noguchi, S. Phase transitions of antibiotic clarithromycin forms I, IV and new form VII crystals. *Int. J. Pharm.* **2018,** *547*, 258-264.

(9) Bobrovs, R.; Kons, A.; Berzins, A.; Rekis, T.; Actins, A. Formation and Transformations of Organic Salt Hydrates: Four Encenicline Hydrochloride Monohydrates and Respective Isostructural Desolvates. *Cryst. Growth Des.* **2018,** *18*, 2100-2111.

(10) Price, C. P.; Glick, G. D.; Matzger, A. J. Dissecting the behavior of a promiscuous solvate former. *Angew. Chem., Int. Ed.* **2006,** *45*, 2062-2066.

(11) Infantes, L.; Fábián, L.; Motherwell, W. D. S. Organic crystal hydrates: what are the important factors for formation. *CrystEngComm* **2007,** *9*, 65-71.

(12) Zong, S. Y.; Wang, J. K.; Xiao, Y.; Sakoth, B.; Wu, H.; Liu, Q.; Zhou, Y. N.; Huang, X.; Hao, H. X. Thermodynamic and population balance models for solvent-mediated phase transformation of lansoprazole. *Chem. Eng. Sci.* **2019,** *207*, 247-257.

(13) Zhang, X.; Yin, Q. X.; Du, W.; Gong, J. B.; Bao, Y.; Zhang, M. J.; Hou, B. H.; Hao, H. X. Phase Transformation between Anhydrate and Monohydrate of Sodium Dehydroacetate. *Ind. Eng. Chem. Res.* **2015,** *54*, 3438-3444.

(14) Bērziņš, A.; Zvaniņa, D.; Trimdale, A. Detailed Analysis of Packing Efficiency Allows Rationalization of Solvate Formation Propensity for Selected Structurally Similar Organic Molecules. *Cryst. Growth Des.* **2018,** *18*, 2040-2045.

(15) Bond, A. D.; Cornett, C.; Larsen, F. H.; Qu, H.; Raijada, D.; Rantanen, J. Structural basis for the transformation pathways of the sodium naproxen anhydrate-hydrate system. *IUCrJ* **2014,** *1*, 328-37.

(16) Braun, D. E.; Bhardwaj, R. M.; Arlin, J. B.; Florence, A. J.; Kahlenberg, V.; Griesser, U. J.; Tocher, D. A.; Price, S. L. Absorbing a Little Water: The Structural, Thermodynamic, and Kinetic Relationship between Pyrogallol and Its Tetarto-Hydrate. *Cryst. Growth Des.* **2013,** *13*, 4071-4083.

(17) Fujii, K.; Aoki, M.; Uekusa, H. Solid-State Hydration/Dehydration of Erythromycin A Investigated by ab Initio Powder X-ray Diffraction Analysis: Stoichiometric and Nonstoichiometric Dehydrated Hydrate. *Cryst. Growth Des.* **2013,** *13*, 2060-2066.

(18) Jia, L.; Zhou, L.; Du, W.; Zhou, L.; Zhang, M.; Hou, B.; Bao, Y.; Wang, Z.; Yin, Q. Simultaneous Effects of Multiple Factors on Solution-Mediated Phase Transformation: A Case of Spironolactone Forms. *Org. Process Res. Dev.* **2018,** *22*, 836-845.

(19) Kons, A.; Bērziņš, A.; Actiņš, A. Polymorphs and Hydrates of Sequifenadine

Hydrochloride: Crystallographic Explanation of Observed Phase Transitions and Thermodynamic Stability. *Cryst. Growth Des.* **2017,** *17*, 1146-1158.

(20) Ahlqvist, M. U. A.; Taylor, L. S. Water diffusion in hydrated crystalline and amorphous sugars monitored using H/D exchange. *J. Pharm. Sci.* **2002,** *91*, 690-698.

(21) Alleso, M.; Tian, F.; Cornett, C.; Rantanen, J. Towards Effective Solid Form Screening. *J. Pharm. Sci.* **2010,** *99*, 3711-3718.

(22) Liu, C. J.; Dang, L. P.; Tong, Y.; Wei, H. Y. Influence of Polymorphs on the Transformation Water Activity of Theophylline. *Ind. Eng. Chem. Res.* **2013,** *52*, 14979-14983.

(23) Zhang, Q.; Mei, X. Two New Polymorphs of Huperzine A Obtained from Different Dehydration Processes of One Monohydrate. *Cryst. Growth Des.* **2016,** *16*, 3535-3542.

(24) Fujii, K.; Uekusa, H.; Itoda, N.; Yonemochi, E.; Terada, K. Mechanism of Dehydration–Hydration Processes of Lisinopril Dihydrate Investigated by ab Initio Powder X-ray Diffraction Analysis. *Cryst. Growth Des.* **2012,** *12*, 6165-6172.

(25) Wang, T.; Du, L.-D.; Wan, D.-j.; Li, X.; Chen, X.-Z.; Wu, G.-F. Retraction of "A New Synthetic Route to Avibactam: Lipase Catalytic Resolution and the Simultaneous Debenzylation/Sulfation". *Org. Process Res. Dev.* **2018,** *22*, 655-655.

(26) Sládková, V.; Skalická, T.; Skořepová, E.; Čejka, J.; Eigner, V.; Kratochvíl, B. Systematic solvate screening of trospium chloride: discovering hydrates of a long-established pharmaceutical. *CrystEngComm* **2015,** *17*, 4712-4721.

(27) Li, H.; Kiang, Y. H.; Jona, J. Multiple approaches to pharmaceutical polymorphism investigation--a case study. *Eur. J. Pharm. Sci.* **2009,** *38*, 426-32.

(28) Xu, Y.; Jiang, L.; Huang, Y.; Wang, J. R.; Mei, X. Solid-state characterization and transformation of various creatine phosphate sodium hydrates. *J. Pharm. Sci.* **2014,** *103*, 3688-3695.

(29) Belenguer, A. M.; Lampronti, G. I.; De Mitri, N.; Driver, M.; Hunter, C. A.; Sanders, J. K. M. Understanding the Influence of Surface Solvation and Structure on Polymorph Stability: A Combined Mechanochemical and Theoretical Approach. *J. Am. Chem. Soc.* **2018,** *140*, 17051-17059.

(30) Christopher P. Price; Adam L. Grzesiak; Matzger, A. J. Crystalline Polymorph Selection and Discovery with Polymer Heteronuclei. *J. Am. Chem. Soc.* **2005,** *127*, 5512 -5517.

(31) Grzesiak, A. L.; Matzger, A. J. New form discovery for the analgesics flurbiprofen and sulindac facilitated by polymer-induced heteronucleation. *J. Pharm. Sci.* **2007,** *96*, 2978-86.

(32) Dolomanov, O. V.; Bourhis, L. J.; Gildea, R. J.; Howard, J. A. K.; Puschmann, H. OLEX2: a complete structure solution, refinement and analysis program. *J. Appl. Crystallogr.* **2009,** *42*, 339-341.

(33) Schefflan, R. *Teach Yourself the Basics of Aspen Plus*; John Wiley & Sons: New Jersey, 2016.

(34) Mahendra G. D.; Pomona, N. Y. Crystalline forms of trans-7-oxo-6-(sulphooxy)-1,6-diazabicyclo[3,2,1]-octane-2-carboxamide sodium salt. U. S. Patent 8,471,025 B2, 2013.

(35) Mahendra G. D.; Pomona, N. Y. Polymorhs and pseudopolymorphs of drug compounds. CN Patent 102834395 B, 2016.

(36) McKinnon, J. J.; Jayatilaka, D.; Spackman, M. A. Towards quantitative analysis of intermolecular interactions with Hirshfeld surfaces. *Chem. Commun.* **2007**, *37*, 3814-3816.

(37) Spackman, M. A.; Jayatilaka, D. Hirshfeld surface analysis. *CrystEngComm* **2009**, *11*, 19-32.

For Table of Contents Use Only

Understanding the role of water in different solid forms of Avibactam sodium and its affecting mechanism

Zhiyong Ding,[†] Wei Su,[†, ‡] Xin huang,[†, ‡] Beiqian Tian,[†] Xiaowei Cheng,[†] Yafei Mao,[†] Guiping Li,[†] Han Liu,[†] and Hongxun Hao[*, †,‡,]

[†] School of Chemical Engineering and Technology, Tianjin University, Tianjin 300072, China

[‡] Collaborative Innovation Center of Chemical Science and Engineering (Tianjin), Tianjin 300072, China

TOC graphic

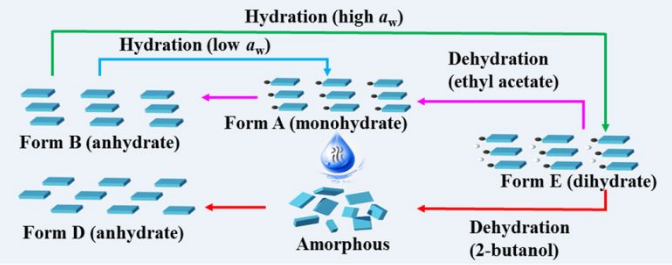

Synopsis

In this study, to reveal the role of water in the formation and dehydration of hydrates, the effect of water activity on the formation of hydrates as well as the mechanism of disintegration of water molecules from crystal lattice was investigated by using Avibactam sodium as model compound.